

Closing Report on ERA-OTKA NN102166 project entitled

“Novel targets and new drug candidates to combat epilepsy: Design of subtype-selective spirobicyclic inhibitors to distinguish among gamma-aminobutyric acid transporter protein subtypes”.

Hungarian PI: Prof Julianna Kardos

Belgian PI: Prof Istvan Marko

Reporting period: 2011-04-01 – 2014-06-30

Summary: Disclosure of LeuT structure, a bacterial orthologue of the SLC6 family member GABA transporter subtypes (GATs) allowed a rapidly advancing global research theme on understanding neurotransmitter- Na^+ symporter function and structure-based drug design. Being funded by the ERA-OTKA research grant, we kept approaching this field by attracting the complementary expertise of Hungarian/Belgian parties for establishing collaboration. Some fundamental topics related to central inhibition through the allosteric modulation of GATs were tackled combining chemical and biological methods. We report on results obtained in the reporting period via the more detailed understanding of GABA- Na^+ symport together with the design and discovery of new potentially selective spirobicyclic GATs inhibitors. Issues were advanced modelling Na^+ symport and allosteric binding in monomeric and dimeric GATs structures, in parallel with the implementation of a three-cycle iterative approach comprising MD, docking, synthesis and efficacy testing of spirobicyclic compounds on HEK293 cell lines expressing the four GATs. Findings answer basic questions on the symport mechanisms of GATs and homologues altogether with the design and discovery of four investigational drugs based on the allosteric selectivity concept. The above combination of theoretical, synthetic and molecular biology techniques provides a powerful tool for finding investigational drugs enabling future development of more specific antiepileptics.

Összefoglalás: SLC6 családba tartozó GABA transzporter altípusok (GATS) bakteriális ortológja, a LeuT szerkezetének felismerése tette lehetővé a neurotranszmitter- Na^+ szimporter funkció megértésén és szerkezetén alapú gyógyszertervezésből kiinduló globális kutatási téma gyors fejlődését. A kutatási területet magyar és belga partnerek szaktudásának kombinálásával, kollaborációban közelítettük - melyet az ERA-OTKA kutatási grant támogatott. GATS allosztérikus modulációjának kombinált kémiai és biológiai megközelítésével a centrális inhibíció alapvető kérdéseit érintettünk. A projekt beszámolóban a GABA- Na^+ szimport mechanizmusának mélyebb megértése továbbá szelektív spirobicyklic GATS inhibitorok tervezése és felismerése útján elért eredményeinkről számolunk be. A spirobicyklic származékok allosztérikus kötődését és a GABA- Na^+ szimportot, monomer továbbá homodimer GATS szerkezetekben modelleztük. Párhuzamosan, tervezés – dokkolás – szintézis – in vitro hatásvizsgálat (GATS-kifejező HEK293 sejtvonalakon) vizsgálatssorozatot valósítottunk meg 3 iterációs ciklusban. Ezen az úton választ kaptunk GATS és homológjaik Na^+ szimport mechanizmusának alapvető kérdéseire, továbbá négy allosztérikus szelektivitás koncepción alapuló, kutatási drog inhibitorok ismertünk fel. Az alkalmazott elméleti, szintetikus és molekuláris biológiai technikák iteratív kombinációja hatékony eszköze lehet a GATS inhibitorok szerkezetén alapuló specifikusabb antiepileptikus gyógyszerek kifejlesztésének a jövőben.

INTRODUCTION

As the main inhibitory neurotransmitter, gamma-aminobutyric acid (GABA) is involved in the regulation of neuronal activity. The excess amount of GABA is taken up by membrane-embedded GABA transporter subtypes belonging to the Na⁺ and Cl⁻ ion-dependent solute carrier family SLC6. Understanding subtype-specific inhibitor efficacy profiles characterized by distinguishable rank order of inhibitor concentrations giving half of substrate transport (IC₅₀ values), and structural measures of selectivity need molecular appreciation of inhibitor-protein interactions. Since crystal structures of GABA transporter subtypes have not been resolved yet, the design of novel, more selective inhibitors requires homology modeling. Homology models of human GATs (hGATs) monomers have previously been built by us and other groups (Palló et al., 2007 and 2009; Wein and Wanner, 2010; Skovstrup et al., 2010) on the basis of the structure of the bacterial orthologue Leu transporter (LeuT) in the “occluded” (Yamashita et al., 2005) conformation representing the substrate activated intermediate state of the alternate access transport mechanism.

Evaluation of *in silico* binding of known GABA analogue substrate inhibitors into the orthosteric, substrate binding crevice of the major, synaptically localized neuronal hGAT1 subtype becomes possible by the observed parallel ranking of docking scores with IC₅₀ values of orthosteric substrate inhibitors (Palló et al., 2007). Extension of the above paradigm over designing allosteric inhibitors of neuronal human BGT-1/mGAT2, as well as glial hGAT-2/mGAT3 and hGAT-3/mGAT4 subtypes has also turned to be viable (Palló et al., 2009; Kragholm et al., 2013; Høg et al., 2006; Kardos et al., 2010). It is concluded that amino acids shaping substrate binding crevices of major neuronal vs. minor glial transporter subtypes are different (Palló et al., 2007 and 2009). By contrast, substrate binding crevices of hGAT-2/mGAT3 and hGAT-3/mGAT4 cannot be distinguished, avoiding sensible prediction of hGAT-2 vs. hGAT-3 selective substrate inhibitors (Kardos et al., 2010).

The allosteric (vestibular) binding crevice of the major transporter subtype hGAT-1/mGAT1 has already been proven to be the target for the antiepileptic drug (AED) Tiagabine (Gabitril®: Tiagabine hydrochloride). In order to overcome potential side effects associated with the use of prescription medicine Gabitril®, such as drowsiness, dizziness and tremor, development of allosteric AED therapeutics acting through minor GABA transporter subtypes, including neuronal hBGT-1/mGAT2 or glial hGAT-2/mGAT3 and hGAT-3/mGAT4 (for the nomenclature *see* Héja et al., 2006) may be conjectured (Kardos et al., 2010; Madsen et al., 2009 and 2011; Schousboe et al., 2011; Vogensen et al., 2013; Smith et al., 2008 and references cited). Therefore we tested the hypothesis that ambient GABA enhancement by selective inhibition of GABA clearance through minor GABA transporter subtypes may provide new AED with less potential side effects. In order to explore this potential, better understanding of mechanisms of GABA-Na⁺ symport and the action of investigational drugs facilitating functional dissection of minor neuronal and glial GABA transporters

are required. In order to develop new, minor GABA transporter subtype target-based allosteric AEDs with less clinical side-effect in the future, we aimed to expand the repertoire of investigational drugs (Héja, 2014; Héja et al., 2012). To this end, clues for an iterative medicinal chemistry approach combining design, synthesis and testing of potential investigational drugs enabling functional dissection of minor GABA transporter subtypes are also binding.

METHODOLOGY

Docking into the allosteric binding crevice of monomeric GABA transporter subtypes. Based on the crystal structure of the occluded conformation of LeuT (Yamashita et al., 2005), basic homology models of GABA transporter subtypes have been built as described previously (Palló et al., 2007 and 2009), using the alignment of Beuming et al. (2006) in combination with the SYBYL molecular energy minimization program package. Briefly, the position of H atoms is arranged first, followed by the side-chains and the backbone atoms. During the preparation of this model, special attention has been paid to the loop regions especially to the most variable EL2 region, located at the extracellular part of the transporters. Initial position of sodium ions Na⁺(1) and Na⁺(2) has been determined by their location in the crystal structure of LeuT. Monomeric homology models were built up in complex with the half-extended pharmacophore conformation of GABA ($\delta(\text{N-C})=4.1\pm 0.4 \text{ \AA}$, $\tau_c=185\pm 15^\circ$; Palló et al., 2007; 2009). Allosteric binding crevice defined as being 10Å around the alpha carbon of vestibular Lys448 and Gln464 in hGAT-1 and hGAT-3, respectively. The raw models have been refined by MD calculations performed at 300K on the ns timescale in explicit membrane and water environment using the CHARMM (ver. c35b4) program package, with the combined protein-lipid force field. To improve model quality, various protein modeling algorithms have also been involved in the preparation, such as Robetta (<http://rosetta.bakerlab.org/>) and Modeller (<http://www.salilab.org/modeller/>). In addition to the occluded conformation of LeuT (Yamashita et al., 2005), the open-to-out conformation (Singh et al., 2008) has also been investigated as a model template in combination with the use of Tiagabine binding crevice identified by Skovstrup et al. (2010) in the open-to-out conformation of hGAT-1 (mGAT1) subtype homology model.

Building up the occluded and the inward open homology models of hGAT-1 homodimer. The model was built from LeuT dimeric crystal structure 2A65 (PDB database) by the Modeller 9.10 program using the alignment of Beuming et al., (2006). In detail, the residues Leu, beta octylglucoside and water were cut out from the structure, only the protein chain and the four sodium ions (two on each side) were retained. The sequence of hGAT1 (SC6A1_HUMAN) was downloaded from SwissProt (UniProtKB/Swiss-Prot code: P30531). This sequence in duplicate was continuously aligned to chain A and chain B of 2A65. The alignment was set manually according to Beuming et al. (2006). The position of the two Na⁺ ions Na⁺(1) and Na⁺(2) were set to be directly taken from the pdb template,

to occupy the same position (coordinates) in the hGAT1 model as in 2A65. Putative disordered regions of hGATs were searched using the IUPRED server, which revealed none or negligible disorder even in the flexible EL2 loop, therefore we found it reliable to include it in the automated modelling procedure. However, to restrict the number of possible conformations, we took advantage of the fact, that the EL2 loop for NSS transporters contain a disulfide bond formed between C164 and C173 (Chen et al., 2007), therefore we integrated Modeller's "DISU patch" (disulfide modelling option) into our modelling routine and set these residues to form disulfide bonds in both chains. The resulting structure from Modeller was obtained in pdb format. Hydrogen atoms and MMFF94 charges were put on this model in SYBYL, where also acetyl and N-methyl groups were placed on the N and C termini. In addition, Cl⁻ ions were added in SYBYL to the suggested binding site (Zomot et al., 2007; Forrest et al., 2007), namely among residues Tyr86, Ser295, Asn327, Ser331. To evaluate molecular motions that can be considered specific for cellular uptake of GABA, we also built an inward open hGAT1 model based on the inward open LeuT variant (pdb code: 3TT3, Krishnamurthy and E. Gouaux, 2012). In contrast to the occluded state LeuT, however, the inward-facing variant was crystallized as a monomer. Therefore the dimeric inward open model was constructed in two steps. First, a dimeric template was built by fitting two 3TT3 monomers on the 2A65 dimer followed by modelling the open-to-in conformation of hGAT1 based on this dimeric template. Neither Na⁺ and Cl⁻ ions, nor GABA were included during the model building. GABA docking to primary orthosteric site S1 in the occluded conformation of the homodimeric hGAT-1 model was performed using the GOLD 4.0 docking program (Cambridge Crystallographic Data Centre Software Ltd., Cambridge, UK). Monomers A and B refer to the chain names in 2A65 dimer. The search space for docking was a 10Å sphere around Na⁺(1) on each side. GABA docking was repeated 10 times and the average of the GOLD scores in 10 runs was used for further analysis. Docked GABA residues were merged to the protein in SYBYL and the structure obtained so far was subjected to molecular dynamics (MD) simulations using the CHARMM modelling package in a 1-palmitoyl-2-oleoylphosphatidyl-choline (POPC) membrane bilayer. In the MD simulations hydrogen atoms were automatically generated and the structures were energy minimized in a protein only environment in 100 steps steepest descent cycles. During the minimization procedure, positions of heavy atoms were kept in place with a harmonic restraining force (first 50 then 10 kcal/mol/Å). Scripts from the CHARMM-GUI membrane builder module were used for the generation, minimization and preproduction equilibration calculations of the hGAT1 in POPC membrane bilayer system. The simulation system comprised 154963 (occluded) and 157649 (inward-facing) atoms consisting of hGAT-1, GABA, POPC, TIP3 water molecules and sodium, potassium and chloride ions. During the constant temperature, pressure and fixed lipid area MD simulations Langevin piston algorithm was used to maintain the temperature at 303K and a pressure of 1atm. The pressure was controlled by the Langevin barostat with a piston collision frequency of 20

ps-1 and the target temperature was kept with the thermal piston mass of $2000\text{kcal}\cdot\text{mol}^{-1}\cdot\text{ps}^2$. Electrostatic interactions were evaluated using the PME method with a grid spacing below 1\AA . The bonds between hydrogen and heavy atoms were constrained with the SHAKE algorithm. In all simulations the all-atom force field CHARMM22 for the protein and CHARMM36 for the lipid atoms (20) were used. The integration time-step was 2.0 fs. Figures were generated using the enhanced perspective option of Pymol. MD simulation time was 13.641 ns. The hGAT-1 backbone atoms RMSD plots during the last 5 ns of the simulation did not show any significant change. For further analysis structures from the last 1 ns simulation were used. Two additional similar MD computations were also performed. In the second simulation (run 2) only the initial random number used at the initial step of the MD simulation was changed. In the third simulation (run 3) the values of the constraining force used during the minimization procedure were doubled compared to original.

Iterative approach elaborated for efficient finding of potentially effective GABA transporter subtype-selective molecules. In order to efficiently conclude on potentially GABA transporter subtype-selective compounds an iterative approach has been developed. Several hits, obtained in the first cycle, have been selected for further syntheses and combined in silico and in vitro evaluation in the descendant cycles. In the reporting period, the approach comprises three cycles of evaluation comprising docking, synthesis and efficacy testing of molecules assessed by the Belgian partner: 1) Potentially effective Tiagabine-analogue spirobicyclic constructs (A-I); 2) Selected synthetic spirobicyclic compounds or precursor fragments (HL series of compounds); 3) Successor variants (ORGA series of compounds). In vitro evaluation of efficacy has been performed on HEK293 cell lines stably expressing mGAT1/hGAT-1, mGAT2/hBGT-1, mGAT3/hGAT-1 and mGAT4/hGAT-3 (Kragholm et al., 2013; Høg et al., 2006; Vogensen et al., 2013). In order to establish predictive in silico methodology, docking score calculations have been compared with in vitro efficacy that are found critical (Palló et al., 2007). Based on previous experience (Palló et al., 2007 and 2009; Nyitrai et al., 2012; Molnár et al., 2008 and 2011; Simon et al., 2004, 2006 and 2008, Szárics et al., 2006 and 2008; Lasztóczy et al., 2006; Kovács et al., 2004; Nyikos et al., 2002), docking score values have been evaluated considering both average score and standard deviation after 10 runs of docking in the allosteric (vestibular or Tiagabine) binding crevices of monomeric occluded or dimeric open-to-out conformations, respectively. All calculations have been carried out using an AMD Opteron cluster of 228 processors.

In silico and in vitro standards. Primary evaluation of in silico docking score values and in vitro efficacy data as well as comparison of in vitro vs. in silico findings has been enabled by applying shared standards with known specificity (**Figure 1**). Two piperidine derivatives, including the hGAT-1 (mGAT1) selective (3R)-1-[4,4-bis(3-methylthiophen-2-yl)but-3-enyl]piperidine-3-carboxylic acid (Tiagabine) and (3S)-1-[2-[(3-methoxyphenyl)-bis(4-methoxyphenyl)methoxy] ethyl] piperidine-3-

carboxylic acid (SNAP-5114) (**Figure 1**) specifically acting on hGAT-2 (mGAT3) and hGAT-3 (mGAT4) subtypes have been used as standards throughout the project. The shared standards (**Figure 1**) serve additional purposes, such as validation/comparison of homology models and docking procedures as well as specificity checking of the GABA transporter subtype-expressing HEK293 cell-lines in course of in vitro efficacy testing.

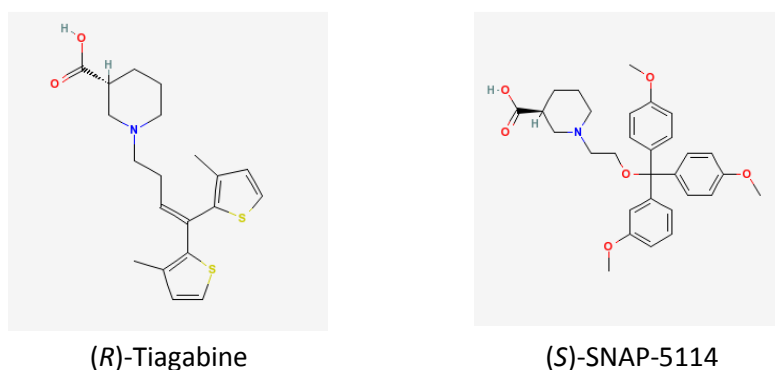


Figure 1. 2D structures of piperidine derivatives applied as standards throughout the project.

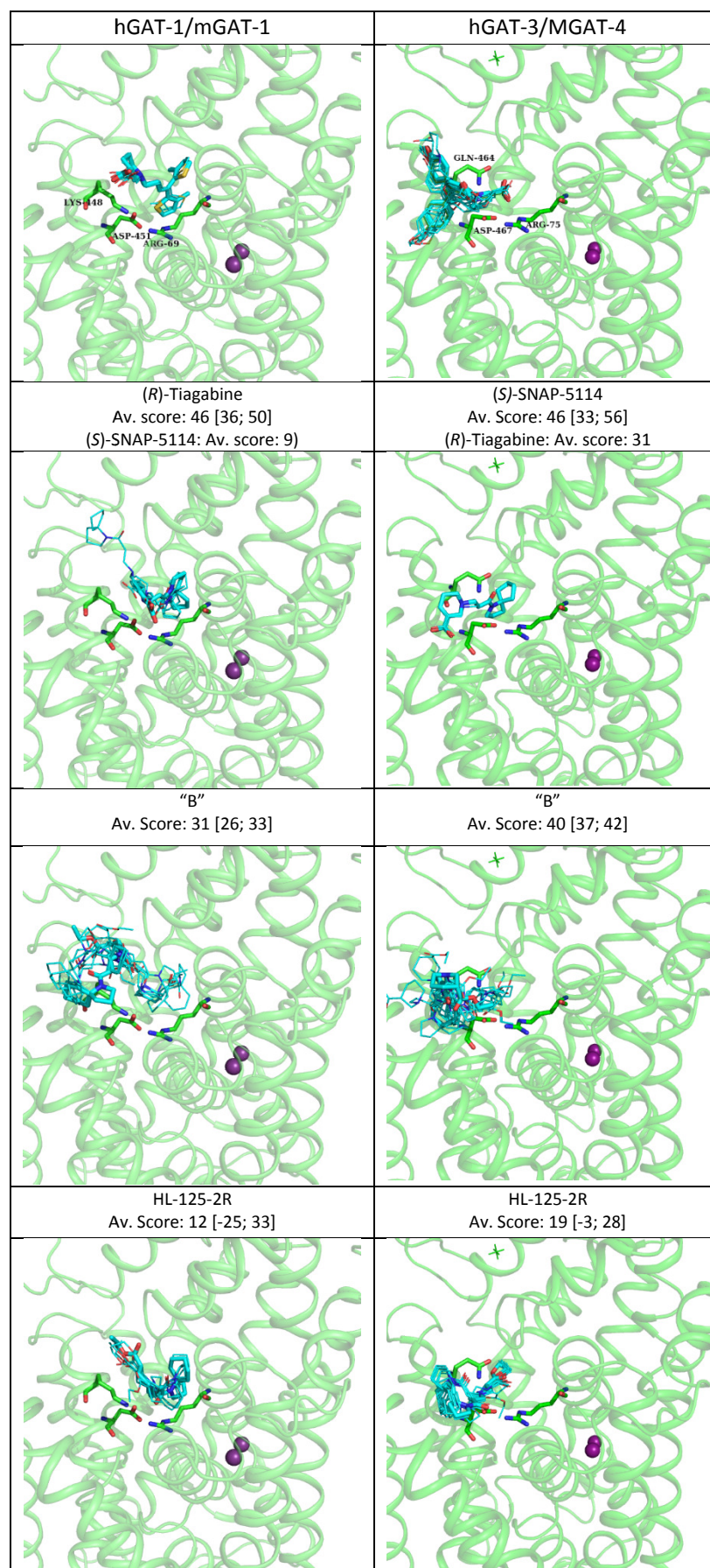
RESULTS

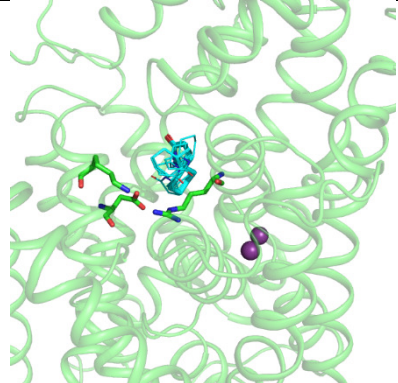
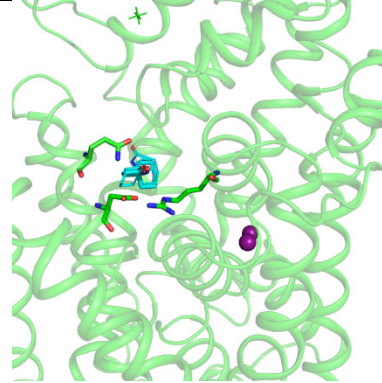
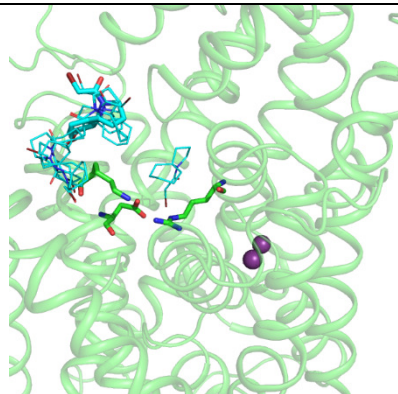
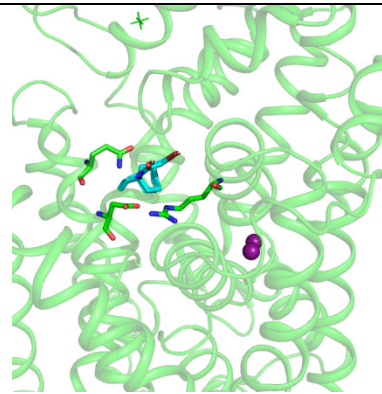
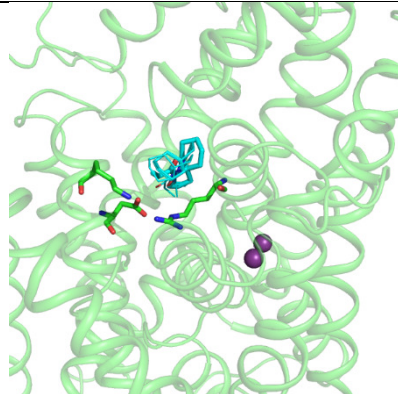
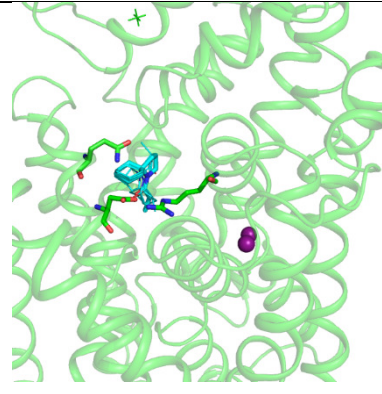
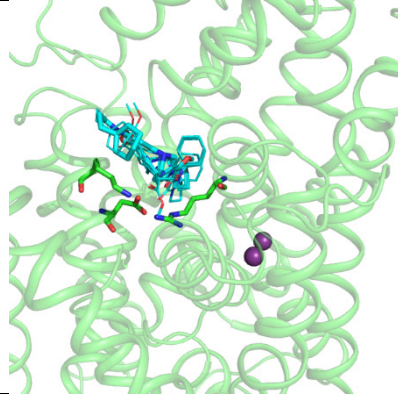
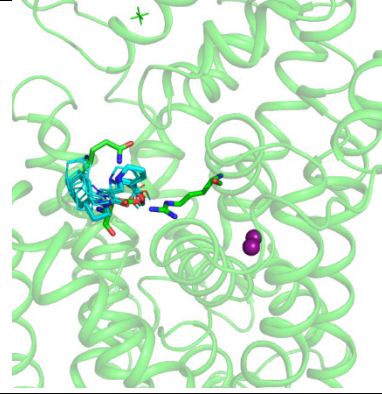
The 1st iteration cycle. Standards (*R*)-Tiagabine and (*S*)-SNAP-5114 (**Figure 1**) together with the initial set of spirobicyclic constructs coded in alphabetical order (**Figure 2**) designed by the Belgian partner were docked into the allosteric binding crevices of the occluded conformations of monomeric hGAT-1 and hGAT-3 homology models. Average score values obtained for docking standards and the designed spirobicyclic constructs into the allosteric (vestibular) binding crevice of hGAT-1 and hGAT-3 are summarized in **Table 1**.

Table 1. Results from docking standards and the initial set of spirobicyclic constructs into the allosteric binding crevices of the occluded conformations of monomeric hGAT-1 and hGAT-3 homology models. Plus and minus signs refer to high and low average score values as characterized by the applied standards, respectively.

Standards and spirobicyclic constructs	hGAT-1	hGAT-3
hGAT-1 selective (<i>R</i>)-Tiagabine	46±2	30±9
hGAT2-2 and hGAT-3 preferring (<i>S</i>)-SNAP-5114	(4±42)	48±3
A	-	-
B	-	+
C	-	-
D	-	-
E	-	+
F	-	+
G	-	-
H	-	-
I	-	-

Average score values for standards follow the order of in vitro efficacy data, however, the high standard deviation indicates that SNAP-5114 fitting the vestibular binding crevice of monomeric



<p>HL-125-2S Av. Score: 1 [-4; 5]</p>	<p>HL-125-2S Av. Score: 33 [17; 40]</p>
	
<p>HL-127-brut Av. Score: 25 [21; 28]</p>	<p>HL-127-brut Av. Score: 32 [31; 33]</p>
	
<p>HL-136-1 Av. Score: 19 [7; 22]</p>	<p>HL-136-1 Av. Score: 33 [30; 35]</p>
	
<p>HL-146-1 Av. Score: 27 [23; 29]</p>	<p>HL-146-1 Av. Score: 30 [27; 33]</p>
	
<p>HL-149-2 Av. Score: -5 [-16; 24]</p>	<p>HL-149-2 Av. Score: 29 [24; 32]</p>

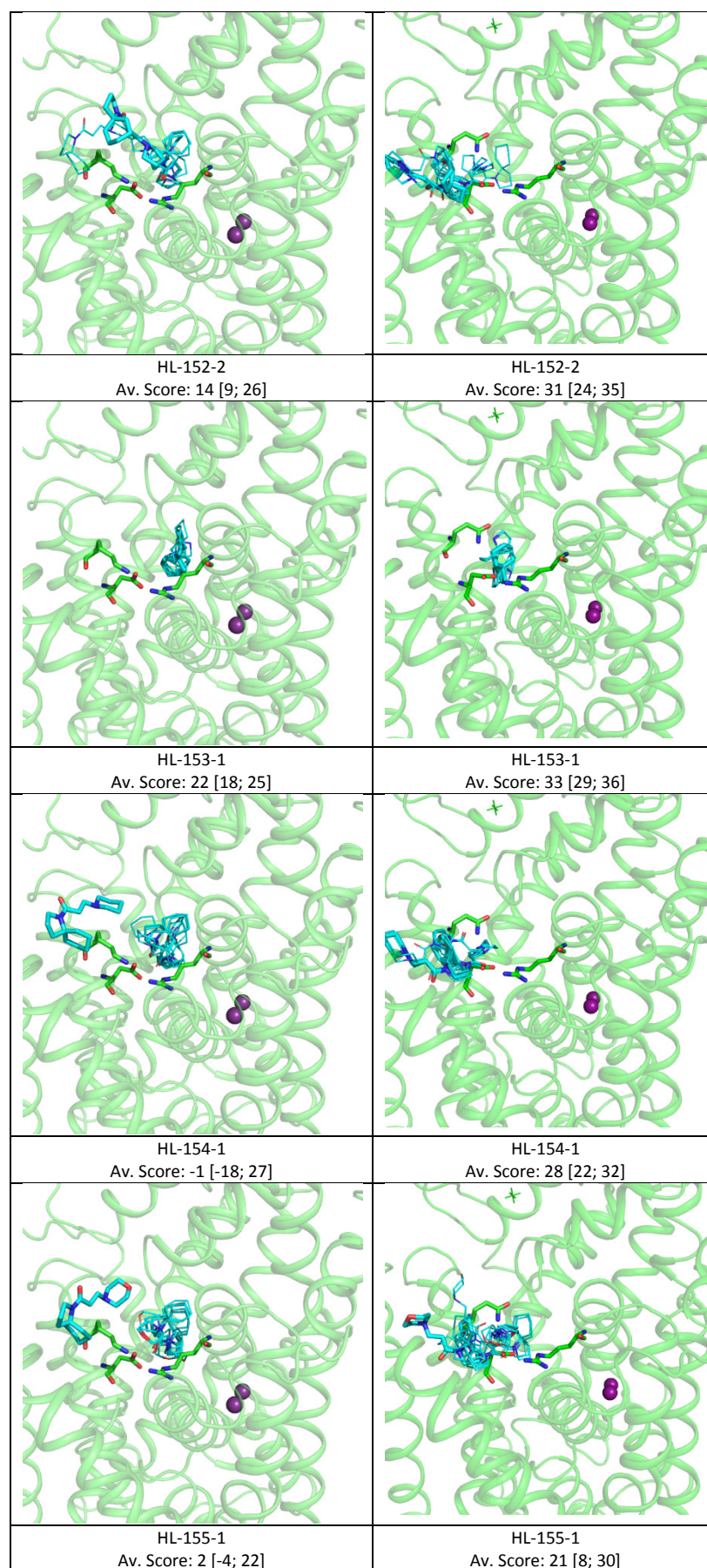


Figure 3. Biasing prediction of binding through variable positions of conformers as given by 10 runs of docking standards, spirobicyclic construct "B" and the HL series of synthetic compounds (light blue) to Lys448 and

Gln464 residues (bright green) in the vestibular binding crevices of hGAT-1/mGAT-1 and hGAT-3/mGAT-4, respectively. The relative position of the orthosteric binding crevices is indicated by Na⁺(1) and Na⁺(2) (violet). By comparison, average scores with minimal and maximal values in brackets are also given.

Table 2. Multiple comparisons of 2D structure, *in silico* docking into the allosteric (Skvostrup et al., 2010) binding crevice of the open-to-out conformation of dimeric homology models of GABA transporter subtypes, in vitro efficacy of the first HL set of synthetic spirobicyclic derivatives and precursors with standards and spirobicyclic construct "B". For binding molecules into the allosteric binding crevices of the occluded conformations of monomeric hGAT-1 and hGAT-3 homology models see **Figure 3**.

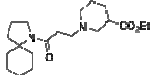
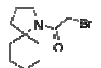
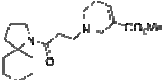
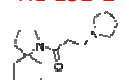
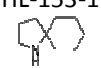
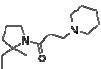
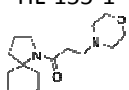
Molecules evaluated	mGAT-1/hGAT-1)		mGAT3/hGAT-2	mGAT-4/hGAT-3	
	Average docking score	Efficacy IC ₅₀ (μM)	Efficacy IC ₅₀ (μM)	Average docking score	Efficacy IC ₅₀ (μM)
(S)-SNAP-5114	9	> 1000	< 10	46 [33; 56]	< 10
(R)-Tiagabine	46 [36; 50]	< 10	> 5000	31	> 5000
"B"	31 [26; 33]	n.d.	n.d.	40 [37; 42]	n.d.
HL-125-2 	1 [-4; 5]	> 5000	5000	33 [17; 40]	> 5000
HL-127-brut 	25 [21; 28]	> 5000	> 5000	32 [31; 33]	> 5000
HL-136-1 	19 [7; 22]	5000	5000	33 [30; 35]	>5000
HL-146-1 	27 [23; 29]	> 5000	5000	30 [27; 33]	> 5000
HL-149-2 	-5 [-16; 24]	> 5000	1000	29 [24; 32]	5000
HL-152-2 	14 [9; 26]	> 5000	5000	31 [24; 35]	1000
HL-153-1 	22 [18; 25]	> 5000	> 5000	33 [29; 36]	> 5000
HL-154-1 	-1 [-18; 27]	> 5000	> 5000	28 [22; 32]	5000
HL-155-1 	2 [-4; 22]	> 5000	> 5000	21 [8; 30]	>5000

Table 3. Comparison of scores obtained by docking standards, spirobicyclic constructs and synthetic **HL** compounds or precursors (fragments) into the allosteric (Skvostrup et al., 2010) binding crevice of the open-to-out conformation of dimeric homology models of GABA transporter subtypes.

Standards Designed constructs "A" – "I" Synthetic HL - compounds	mGAT-1/hGAT-1 chain A	mGAT3/hGAT-2 chain B	mGAT-4/hGAT-3 chain B
(<i>R</i>)-Tiagabine	50 ± 1	51 ± 6	45 ± 5
(<i>S</i>)-SNAP-5114	29 ± 2	39 ± 4	54 ± 4
A	34 ± 5	23 ± 6	26 ± 6
B	33 ± 5	25 ± 7	34 ± 6
C	36 ± 3	38 ± 3	28 ± 12
D	34 ± 5	25 ± 10	33 ± 6
E	37 ± 4	26 ± 4	33 ± 7
F	39 ± 5	29 ± 9	38 ± 4
G	40 ± 4	7 ± 14	38 ± 5
H	27 ± 3	26 ± 11	29 ± 5
I	29 ± 6	25 ± 12	32 ± 5
HL-125-2	38 ± 5	(22 ± 16)	39 ± 4
HL-127_brut	31 ± 1	28 ± 1	25 ± 1
HL-136_1	32 ± 1	29 ± 1	29 ± 1
HL-146_1	34 ± 1	31 ± 1	31 ± 1
HL-149_2	35 ± 5	14 ± 6	32 ± 5
HL-152_2	34 ± 2	29 ± 5	35 ± 2
HL-153_1	30 ± 1	29 ± 1	28 ± 1
HL-154_1	36 ± 4	28 ± 8	32 ± 2
HL-155_1	37 ± 1	15 ± 7	31 ± 2

The third iteration cycle. Synthetic (**ORGA**) series of spirobicyclic compounds (for their 2D structures see **Figure 4**) assessed by the Belgian partner were tested for in silico binding (**Table 4**) and in vitro efficacy (**Table 5, Figure 5**). Initial screening of the 19 **ORGA** compounds has been assessed by determination of specific [³H]GABA uptake in the presence of the **ORGA** compounds applied in three concentrations: 10 μM, 100 μM and 1000 μM. Lower values have been found for ORGA-5 and ORGA-6 acting at mGAT-2/hBGT-1 (**Table 4**), suggesting that these spirobicyclic derivatives may possibly be selective inhibitors of minor, neuronal hBGT-1 (human betain) subtype. IC₅₀ values have also been determined (**Figure 5**) indicating approximately one order of magnitude higher efficacy when **HL** compounds in **Table 2** are compared.

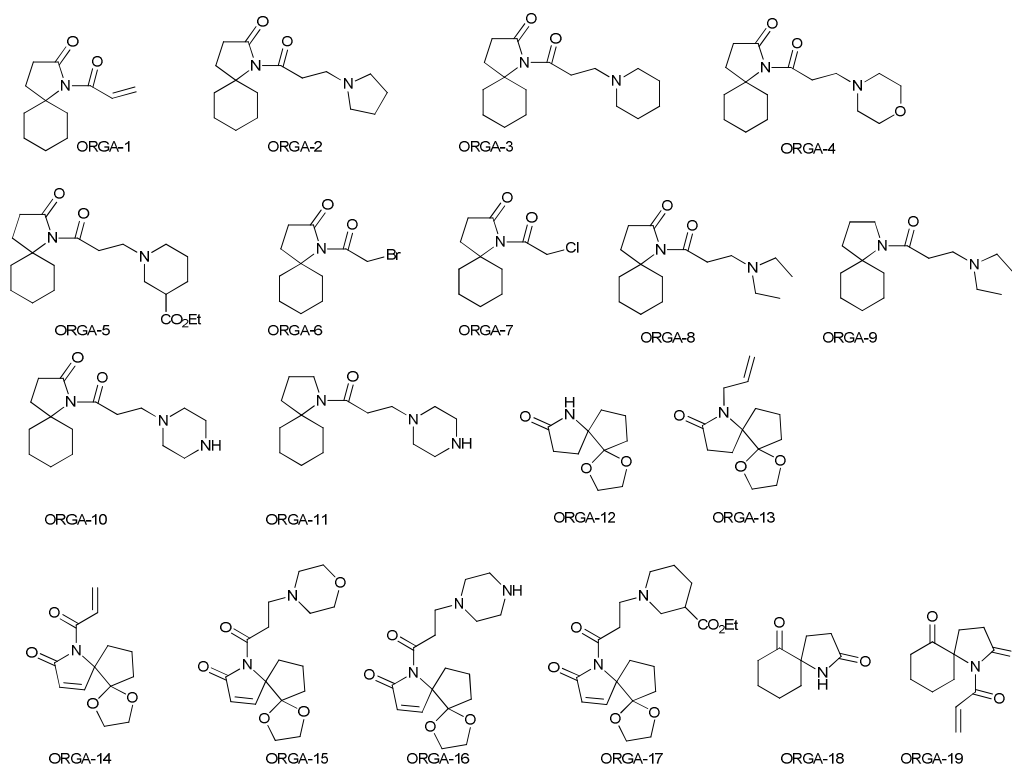


Figure 4. 2D structures of the ORGA-1-19 series of compounds

Table 4. Scores for docking standards and ORGA-1-19 spirobicyclic derivatives into the allosteric (Skovstrup) binding crevice of the open-to-out conformations of the dimeric hGAT homology models subtype

allosteric (Skovstrup) binding crevice	hGAT-1 (chain A)	hGAT-2 (chain B)	hGAT-3 (chain B)
(R)-Tiagabine	52.6 ± 3.7	52.0 ± 5.2	46.3 ± 6.4
(S)-SNAP	29.0 ± 22.0	38.1 ± 13.0	58.0 ± 8.8
ORGA-1	35.2 ± 0.4	34.7 ± 0.8	34.5 ± 0.3
ORGA-2	33.7 ± 5.0	30.9 ± 5.6	32.7 ± 9.9
ORGA-3	37.0 ± 1.0	43.0 ± 3.0	38.6 ± 1.7
ORGA-4	34.8 ± 2.1	24.1 ± 3.9	31.8 ± 3.0
ORGA-5	43.7 ± 2.9	(30.0 ± 14)	43.9 ± 4.2
ORGA-6	35.1 ± 0.4	33.7 ± 0.8	34.4 ± 0.4
ORGA-7	34.8 ± 0.7	33.1 ± 1.1	33.4 ± 0.9
ORGA-8	32.5 ± 2.2	26.6 ± 3.5	29.8 ± 4.5
ORGA-9	26.1 ± 6.5	20.5 ± 4.0	25.9 ± 1.6
ORGA-10	37.6 ± 1.0	31.3 ± 5.9	35.5 ± 7.7
ORGA-11	32.2 ± 1.5	21.4 ± 8.7	28.8 ± 1.9
ORGA-12	31.6 ± 0.3	30.6 ± 1.1	27.6 ± 1.5
ORGA-13	40.1 ± 2.0	31.7 ± 1.6	33.7 ± 0.9
ORGA-14	36.9 ± 1.7	37.9 ± 0.3	32.2 ± 0.6

ORGA-15	42.8 ± 4.2	29.1 ± 10.2	36.8 ± 1.1
ORGA-16	41.2 ± 5.0	47.4 ± 11	36.2 ± 3.1
ORGA-17	41.5 ± 3.8	25.6 ± 5.8	45.9 ± 3.1
ORGA-18	31.3 ± 0.6	31.2 ± 0.3	27.1 ± 1.1
ORGA-19	34.4 ± 1.3	35.6 ± 0.3	31.2 ± 0.5

Table 5. Initial screening of the 19 ORGA compounds in 10 µM, 100 µM and 1000 µM. Values represent specific [³H]GABA uptake in the presence of the test compounds. Lower values mean more effective inhibition.

	Specific [³ H]GABA uptake (%)											
	mGAT1 (hGAT-1)			mGAT2 (hBGT-1)			mGAT3 (hGAT-2)			mGAT4 (hGAT-3)		
	10 µM	100 µM	1000 µM	10 µM	100 µM	1000 µM	10 µM	100 µM	1000 µM	10 µM	100 µM	1000 µM
ORGA-1	96 ±3	98 ±4	90 ±1	89 ±3	95 ±4	94 ±16	92 ±1	97 ±1	99 ±9	93 ±0	98 ±6	95 ±3
ORGA-2	97 ±4	86 ±8	96 ±2	86 ±8	71 ±10	87 ±8	104 ±1	94 ±0	90 ±2	95 ±2	89 ±3	89 ±4
ORGA-3	103 ±1	101 ±2	92 ±10	105 ±2	101 ±3	87 ±3	98 ±5	100 ±2	91 ±3	102 ±5	101 ±1	96 ±2
ORGA-4	94 ±1	104 ±1	98 ±5	102 ±5	96 ±4	89 ±9	96 ±2	106 ±0	97 ±3	100 ±3	79 ±20	96 ±1
ORGA-5	101 ±3	87 ±4	85 ±5	99 ±1	80 ±2	47 ±9	99 ±7	85 ±2	77 ±14	104 ±3	91 ±1	88 ±2
ORGA-6	90 ±4	90 ±3	93 ±5	89 ±1	87 ±3	48 ±11	93 ±7	83 ±8	77 ±14	92 ±3	90 ±1	96 ±1
ORGA-7	94 ±3	95 ±4	79 ±16	99 ±1	113 ±13	99 ±14	97 ±2	96 ±2	91 ±5	99 ±2	96 ±1	92 ±2
ORGA-8	104 ±3	101 ±1	93 ±1	100 ±4	104 ±8	98 ±15	108 ±1	100 ±1	98 ±1	101 ±3	98 ±1	89 ±6
ORGA-9	106 ±5	101 ±4	95 ±3	96 ±3	91 ±3	72 ±10	99 ±2	98 ±1	93 ±4	103 ±3	98 ±1	93 ±5
ORGA-10	102 ±3	93 ±10	97 ±6	90 ±2	91 ±8	85 ±10	101 ±3	103 ±2	100 ±2	97 ±3	98 ±1	96 ±4
ORGA-11	102 ±3	94 ±2	95 ±7	107 ±3	100 ±1	67 ±7	101 ±3	98 ±2	104 ±19	100 ±3	96 ±4	88 ±2
ORGA-12	96 ±1	93 ±0	100 ±3	104 ±4	101 ±6	97 ±3	96 ±4	93 ±5	102 ±1	100 ±1	98 ±2	100 ±1
ORGA-13	94 ±2	97 ±13	102 ±6	99 ±7	102 ±2	81 ±6	94 ±1	95 ±4	102 ±3	107 ±12	104 ±1	111 ±11
ORGA-14	100 ±2	98 ±7	102 ±1	92 ±9	106 ±2	104 ±5	99 ±1	101 ±3	107 ±3	97 ±2	103 ±3	109 ±2
ORGA-15	103 ±9	100 ±5	100 ±4	124 ±13	100 ±5	101 ±2	109 ±2	93 ±3	99 ±4	105 ±3	99 ±1	102 ±2
ORGA-16	104 ±4	107 ±6	118 ±12	108 ±0	110 ±4	105 ±1	106 ±0	100 ±4	102 ±3	106 ±1	106 ±5	104 ±0
ORGA-17	102 ±4	103 ±3	94 ±7	103 ±6	83 ±1	73 ±1	103 ±3	99 ±1	89 ±5	104 ±1	99 ±2	97 ±6
ORGA-18	107 ±2	99 ±7	105 ±3	105 ±5	108 ±4	113 ±8	100 ±1	101 ±2	99 ±1	96 ±1	99 ±3	101 ±1
ORGA-19	101 ±5	98 ±3	98 ±1	99 ±5	113 ±8	117 ±12	100 ±2	90 ±4	97 ±5	99 ±2	102 ±1	95 ±1

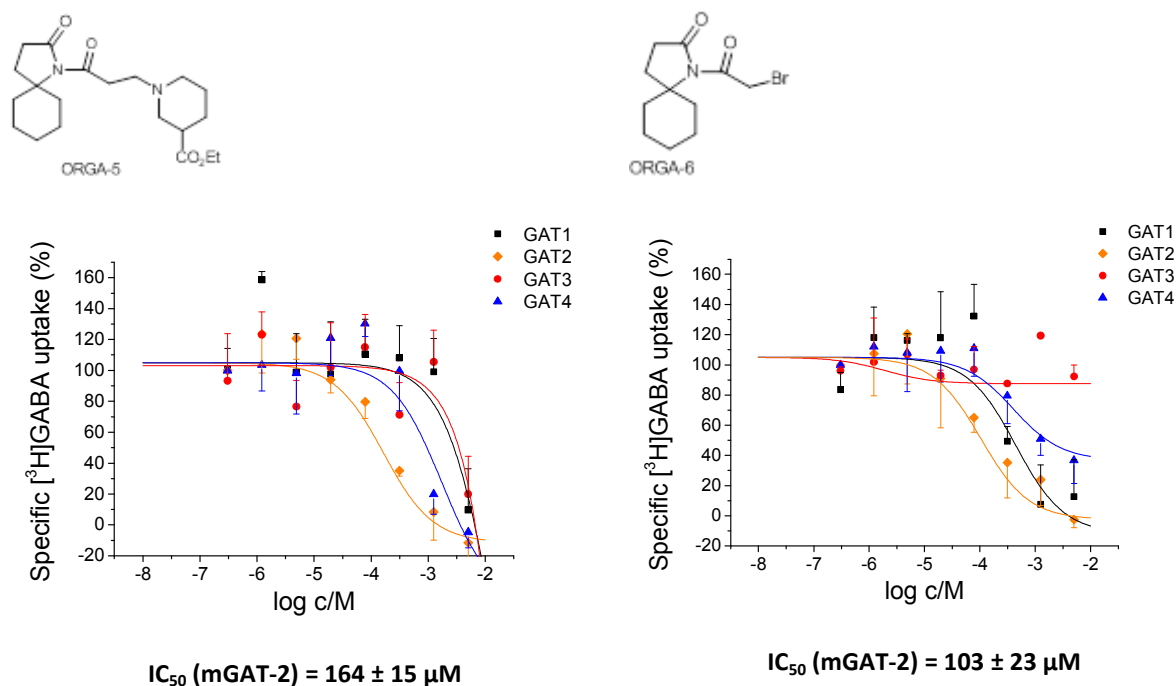


Figure 5. IC_{50} determination for ORGA-5 and ORGA-6 assayed by the mGAT1, mGAT2, mGAT3 and mGAT4 subtype expressing cell lines.

Molecular understanding of GABA- Na^+ symport function in the occluded conformation of homodimeric hGAT-1 subtype homology model. GABA transporter subtype hGAT-1 was homology modeled in the occluded state as a dimer. MD simulations have been started on the whole dimeric form in implicit membrane (1024 amino acid residues, 1 GABA molecule, 2 Na^+ ion and 33 water molecules in each monomeric units, called chains A and B). In the binding crevice of the $Na^+(2)$ ion, 1-3 stabilization centre elements appear among G59, I62, L392, A395, S396 residues, suggesting that the $Na^+(2)$ ion and its binding crevice may play a stabilizing role for the intermediary state of the transport taking place *via* the alternate access mechanism. After short MD simulation (< 10ns) GABA adopts a ring-like conformation characterized by the following average distances: $d(N-O) = 3 \text{ \AA}$, $d(Na^+(1)-O) = 2 \text{ \AA}$, where N is the nitrogen atom of the amino group and O is one of the carboxyl oxygen atoms of GABA. These data indicate the early formation of ring-like GABA conformation by intramolecular H-bonding between terminal N and O atoms of terminal amino and carboxy groups of GABA. Characterized by short N-O and $Na^+(1)-O$ distances, it is plausible that the intramolecular H-bonding is stabilized by the nearby $Na^+(1)$. Based on the above findings and additional theoretical calculations demonstrating that the $Na^+(1)$ facilitated formation of H-bridged ring-like GABA is energetically favorable we hypothesized that the ring-like GABA leave the transporter in complex with $Na^+(1)$.

This way, the formation of $Na^+(1)$ bridged ring-like GABA may be a critical elementary step that couple downhill flux of sodium ion to uphill transport of GABA, not distinguished as yet.

Simulations performed in the 1-10 ns range of time elucidated persistent formation of half-extended minor and H-bridged major GABA conformations, referred to as binding and traverse conformations, respectively. The traverse GABA conformation was further stabilized by the orthosteric binding crevice-bound $\text{Na}^+(1)$. We also observed $\text{Na}^+(1)$ translocation to hGAT-1-bound Cl^- in addition to the appearance of water molecules at GABA and around the protein-bound $\text{Na}^+(2)$, conjecturing causality. Scaling transporter dynamics have been disclosed, suggesting that the traverse GABA conformation may be valid for developing substrate inhibitors with high efficacy. The potential for this finding is significant with impact not only in designing GABA transporter inhibitors but wherever, understanding alternate access mechanisms of neurotransmitter-sodium symporters is valuable.

CONCLUSIONS

Major findings of the project entitled “Novel targets and new drug candidates to combat epilepsy: Design of subtype-selective spirobicyclic inhibitors to distinguish among gamma-aminobutyric acid transporter protein subtypes” are *i)* the design of 9 spirobicyclic constructs and the selection for synthesis of “B”, “E”, “F and “G” derivatives, based on docking into the allosteric binding crevice of monomeric and homodimeric GAT subtype-models, respectively;; *ii)* the synthesis of 9 spirobicyclic HL compounds and precursors (fragments) characterized by millimolar efficacy and mGAT-3/hGAT-2 (**HL-149-2**) vs. mGAT-3/hGAT-3 (**HL-152-2**) subtype-selectivity; *iii)* the synthesis of 19 spirobicyclic ORGA compounds characterized by order of magnitude higher efficacy displaying subtype-selectivity order mGAT-2/hBGT-1 > mGAT-4/hGAT-3 >> mGAT-1/hGAT-1 \approx mGAT-3/hGAT-2 (**ORGA-5**) vs. mGAT-2/hBGT-1 > mGAT-1/hGAT-1 > mGAT-4/hGAT-2 >> mGAT-3/hGAT-2 (**ORGA-6**); *iv)* the potential of gradual tuning through derivatives of the more stringently fitting spirobicyclic construct "G", that may possibly superior the recently described guanidino-derivative of 2-amino-1,4,5,6-tetrahydropyrimidine-5-carboxylic acid (Al-Khawaja et al., 2014); *v)* the description of sodium-assisted formation of binding and traverse conformations of GABA in the homodimeric hGAT-1 homology model. Growing awareness of osmolyte betain may play in normal and diseased function of the brain kidney and liver (for a review see Kempson et al, 2014), including hepatitis C virus infection (Satoh et al, 2011), vision (Garrett et al., 2013), human breast cancer metastases to the brain (Neman et al., 2013) invites furthering of our medicinal chemistry approach, aimed at finding GABA transporter subtype-selective investigational drugs. Based on structures of Vertex’s Lumacaftor/VX-809 (Van Goor et al., 2011) now in clinical trial phase III or other investigational drugs correcting cystic fibrosis protein (Odolczik et al., 2013), we may anticipate that some of our spirobicyclic compounds or further derivatives have the potential to correct cystic fibrosis protein disfunctioning.

GRANT ACKNOWLEDGEMENTS:**Lectures, Abstracts and submitted or in preparation articles**

1. Simon Á. Molecular modelling of GABA transporter function, presentation at the Department of Pharmazie, Zentrum für Pharmaforschung, Ludwig-Maximilians-Universität, München, May 12, 2011.
2. Simon Á, Bencsura Á, Kardos J. Molecular modeling of gamma-aminobutyric acid transporter function, poster at the Fourth SFB35 Symposium on Transmembrane Transporters in Health and Disease, Vienna, Sept 8-9, 2011.
3. Simon Á, Bencsura Á, Kardos J, Modeling gamma-aminobutyric acid transporter function, presentation at the Chemical Research Centre – Research Days, Budapest, Nov 22-24, 2011.
4. Kardos J, Héja L, Nyitrai G, Kékesi O, Simon Á, Bencsura Á. Glial GABA transporters: function and modeling, presentation at the Conference of the Hungarian Biochemical Society Pécs, Aug 28-31, 2011.
5. Simon Á, Bencsura Á, Mayer I, Kardos J. Homology modelling of gamma-aminobutyric acid transporter dimers in the occluded and inward open states, poster at the Fifth SFB35 Symposium on Transmembrane Transporters in Health and Disease, Vienna, Sept 24-25, 2012.
6. Simon Á, Bencsura Á, Mayer I, Kardos J. Homology modelling of gamma-aminobutyric acid transporter dimers in the occluded and inward open states, “excellent” presentation at the Chemical Research Centre – Research Days, Budapest, Nov 27-29, 2012.
7. Kardos J, Héja L. Therapeutic potential of neuro-glia coupling in epilepsy. Invited lecture at the 5th ICDDT, Dubai, 2013.
8. Héja L. Astrocytes convert network excitation to tonic inhibition of neurons, invited lecture presented at the 11th European Meeting on Glial Cell Function in Health and Disease, Jul 03-06, 2013, Berlin, GLIA 61, S27, 2013.
9. Pál I, Nyitrai G, Kardos J, Héja L. Glial and neuronal mechanisms underlying the label-free intrinsic optical signal, poster presented at the 11th European Meeting on Glial Cell Function in Health and Disease, Jul 03-06, 2013, Berlin, GLIA 61, S108, 2013.
10. Kékesi O, Nyitrai G, Szabó P, Fiáth R, Ulbert I, Kardos J, Héja L. Glial GABA transporters downregulate enhanced neuronal activity, poster presented at the 11th European Meeting on Glial Cell Function in Health and Disease, Jul 03-06, 2013, Berlin, GLIA 61, S122, 2013.
11. Kékesi O, Kardos J, Héja L. Astrocyte calcium dynamics reveal neuro-glia coupling during recurrent epileptiform discharge, poster to be presented at the 7th SFB35 Symposium, Transmembrane Transporters in Health and Disease, Vienna, Sept 24-25, 2014.
12. Simon Á, Bencsura Á, Héja L, Magyar Cs, Kardos J. Sodium-assisted formation of binding and traverse conformations of the substrate in a neurotransmitter sodium symporter model. CDDT *submitted*.
13. Kékesi O, Kardos J, Héja L. Astrocyte calcium dynamics manifest bidirectional dynamical coupling of astrocytes with neurons in course of recurrent discharges in an in vitro model of pharmacoresistant temporal lobe epilepsy. GLIA, *submitted*.
14. Kardos J, Héja L. Universality of alternate access mechanisms: Scaling transporter dynamics. TRENDS IN PHARMACOLOGICAL SCIENCE, *in preparation*.
15. Kardos J, Héja L, Simon Á, Kékesi O, Fekete E, Markó I. Design, homology modelling, synthesis and in vitro evaluation of spirocyclic derivatives for selectivity at *human GABA transporter* subtypes. EMBO MOLECULAR MEDICINE, *in preparation*.

Papers appeared with the acknowledgement of the grant: 1. Héja L. Astrocytic target mechanisms in epilepsy. CURRENT MEDICINAL CHEMISTRY 21, 755-763 (2014) IF: 4.070; 2. Héja L, Nyitrai G, Kékesi O, Dobolyi A, Szabó P, Fiáth R, Ulbert I, Pal-Szenthe B, Palkovits M, Kardos J. Astrocytes convert network excitation to tonic inhibition of neurons. BMC BIOLOGY 10, 26 (2012) IF:6.531, Cit:15; 3. Okiyoneda T, Veit G, Dekkers JF, Bagdany M, Soya N, Xu H, Roldan A, Verkman AS, Kurth M, Simon Á, Hegedus T, Beekman JM, Lukacs GL. Mechanism-based corrector combination restores $\Delta F508$ -CFTR folding and function. NATURE CHEMICAL BIOLOGY 9, 444-454 (2013) IF: 12.948, Cit:10; 4. Pál I, Nyitrai G, Kardos J, Héja L. Neuronal and astroglial correlates underlying spatiotemporal intrinsic optical signal in the rat hippocampal slice. PLOS ONE 8, e57694 (2013) IF:3.730; 5. Nyitrai G, Keszthelyi T, Bóta A, Simon Á, Tőke O, Horváth G, Pál I, Kardos J, Héja L. Sodium selective ion channel formation in living cell membranes by polyamidoamine dendrimer. BIOCHIMICA ET BIOPHYSICA ACTA (BBA) - BIOMEMBRANES 1828, 1873-1880 (2013) IF:3.389; 6. Nyitrai G, Héja L, Jablonkai I, Pál I, Visy J, Kardos J. Polyamidoamine dendrimer impairs mitochondrial oxidation in brain tissue. JOURNAL OF NANOBIO TECHNOLOGY 11, 9 (2013) IF:-; 7. Nyitrai G, Kékesi O, Pál I, Keglevich P, Csiki Z, Fügedi P, Simon Á, Fitos I, Németh K, Visy J, Tárkányi G, Kardos J. Assessing toxicity of polyamidoamine dendrimers by neuronal signaling functions. NANOTOXICOLOGY 6, 576-586 (2012) IF:7.844 Cit:7